Rapid RFID Location and Orientation Recovery

by

Nicholas Stearns Selby

Submitted to the Department of Mechanical Engineering
in partial fulfillment of the requirements for the degree of

Master of Science in Mechanical Engineering

at the

MASSACHUSETTS INSTITUTE OF TECHNOLOGY

June 2018

Author . . . .
Department of Mechanical Engineering
March 16, 2018

Certified by. . . . .
Fadel Adib
Assistant Professor of Media Arts and Sciences
Thesis Supervisor

Certified by. . . . .
Sanjay Sarma
Professor of Mechanical Engineering
Thesis Reader

Accepted by . . . .
Rohan Abeyaratne
Chairman, Department Committee on Graduate Theses

Rapid RFID Location and Orientation Recovery

by

Nicholas Stearns Selby

Submitted to the Department of Mechanical Engineering
on March 16, 2018, in partial fulfillment of the
requirements for the degree of
Master of Science in Mechanical Engineering

Abstract

This thesis aims to enable virtual and augmented reality (VR/AR) systems to track objects accurately through occlusions via RFID localization. Currently, three major obstacles prevent the use of RFID localization in VR/AR systems: (1) there exists a trade-off between measurement speed and ability to deal with multipath, so systems which can produce accurate results either require a highly constrained environment or several seconds to localize; (2) past RFID localization techniques lack robustness to changes in tag orientation; and (3) current RFID orientation extraction methodologies are largely inaccurate. To overcome these challenges, this thesis presents RF-Reality, a new system that leverages a novel OFDM backscatter technique and differential channel estimation algorithm to perform accurate, rapid RFID position and orientation recovery.

Thesis Supervisor: Fadel Adib
Title: Assistant Professor of Media Arts and Sciences

Disclaimer

The work in this thesis was performed in collaboration with a postdoc, Yunfei Ma, and two other students, Zhihong Luo and Manish Singh, all in the Signal Kinetics research group at the MIT Media Lab. Most of the techniques in this thesis were developed during discussions and brainstorming sessions with the collaborators. We all share credit for the design and the system architecture. We also share credit in implementing and evaluating the low latency and high frame rate techniques. My role extended beyond the design and high-frame rate implementation to implementing and evaluating the orientation-independent localization and orientation extraction.

Acknowledgments

Contents

List of Figures

Chapter 1

Introduction

Radio Frequency Identifier (RFID) technology is a powerful tool typically used to automatically identify tags attached to objects. These tags can be battery- and maintenance-free, cost on the order of pennies per tag, and come in the form of small, non-intrusive stickers which can be easily attached to almost any object. RFID tags are rapidly becoming ubiquitous; they are currently used in manufacturing to track objects on assembly lines [43], in warehouses to record inventory [41], and in retail stores to monitor clothing [71]. Current estimates of the global RFID market place its value at 16 billion dollars [49] with a projected growth to 24 billion dollars by 2020 [30].

Academia has also taken great interest in RFID localization [15, 53, 60, 68, 69, 74]. RFID localization research has become increasingly popular for the following reasons:

- **Built-In Identification.** Unlike vision-based localization systems which require special training to identify an object by its appearance [63, 22, 38], RFID technology has a built-in mechanism to easily communicate a unique identifier from the tag to the reader, allowing for immediate identification of tags without the need for computationally expensive training algorithms.

- **Low Cost.** Widely deployed RFIDs such as Alien Squiggle [13], Omni-ID Exo [55], and Smartrac [64] cost 5-10 cents per tag. They require no maintenance or battery [13, 55, 64].

- **Non-Line-of-Sight.** When visible light comes into contact with a solid object like a wall or box, it scatters. This severely limits vision-based localization systems to only be able to find objects with an unobstructed line of sight to the tracking device. Due to their longer wavelength, RF signals like those used by RFID tags and readers can traverse occlusions, allowing a reader to query tags even when a camera could not see them.

This thesis presents RF-Reality, a system that enables virtual and augmented reality systems to take advantage of the benefits of RFID localization.

1.1 An Opportunity for Virtual and Augmented Reality

This thesis enables rapid location and orientation sensing of RFID tags for use in new virtual and augmented reality applications. Today's VR/AR systems such as Sony's PlayStation VR [65], the HTC Vive [27], and Facebook's Occulus Rift [54] all rely on vision-based localization technology and thus forego all of the RF advantages described above. An RF-based VR/AR system would fundamentally alter the way in which users interact with the internet of things, enabling tracking for a virtually limitless quantity of objects with no need for prior training or expensive markers even if the tracked objects are occluded from view.

Furthermore, we aim to leverage the built-in identification of RFID stickers to allow users to interact with the entire internet of things via a fundamentally more expressive interface. Specifically, we aim to enable skeletal tracking by attaching RFID's to user limbs, then taking advantage of RFID's built-in identification to map each response to its respective limb for tracking. This would enable functionality similar to the XBox Kinect [10], but with the added ability to track users which are hidden behind furniture or in cluttered environments. RFID's unique mapping can also be used to leverage multi-user interactions in games like collaborative challenges and keeping score.

Because RFID's cost just cents per tag, they can also enable rapid expansion of the internet of humans and things. RFID's placed on objects can enable interactions in augmented reality by understanding with what a user interacts and the exact timing and nature of that interaction. Such a capability would enable shopping analytics in retail stores, live feedback on the handling of tools and parts on a factory floor, and more interactive training in hands-on education.

1.2 Challenges

However, despite the advantages of RF localization, state-of-the-art RF localization techniques have exhibited several limitations for commercial adoption. Namely:

- **Latency, Frame Rate, and Motion.** Currently, there exists a trade-off between measurement speed and the generality of environments with which past techniques can operate. Systems which can provide accurate results either require a highly constrained environment [69, 74] or have frame rates of less than 1 Hz [45]. However, user studies in VR/AR systems have shown users require a tracking latency of less than 20 milliseconds to avoid motion sickness [39, 50, 56]. If such a method were immediately employed in a VR system today, users would experience severe discomfort.

- **Orientation Dependence.** While techniques to localize RFID's regardless of orientation do exist, such methods either lack robustness to multipath by relying on received signal strength (RSSI) [48, 47, 61] or rely on multiple RFID's to be fixed on a single rigid body [68, 62, 24, 26]. Current techniques which

14

accurately estimate the position of a single RFID tag can only do so if the tag's orientation remains constant with respect to the reader or if several other constrained RFID's are placed in the environment. Without these constraints, changes in orientation can cause errors in position. Because many VR applications require tracking of natural movement of user limbs and other objects, this dependence on orientation would create many problems for a complete system.

- **Lack of Orientation Extraction.** Using RFID's to determine an object's orientation is not new, but, as above, current systems which do so either assume a dominant line-of-sight between the reader and tag [61], or require the use of multiple tags to be placed on each rigid body to be tracked [68, 62, 24, 26]. Even if rapid, orientation-independent RFID localization were implemented with the same performance as popular vision-based systems, orientation could only be recovered by placing multiple tags on an object, then using their locations relative to each other to extract orientation data.

1.3   Organization

The remainder of the thesis will be organized as follows: Chapter 2 will explore the state-of-the-art in both VR/AR systems as well as RF localization. Chapters 3, 4, and 5 will discuss and demonstrate solutions to the challenges listed above, with each chapter respectively answering the issues of latency, orientation dependence, and orientation extraction. Finally, Chapter 6 will conclude with a discussion of applications and future work.

Chapter 2

Related Work

Related work in this area can be broadly characterized in four main areas: ultrawideband (UWB) tags, virtual and augmented reality (VR/AR) systems, radio frequency (RF) localization, and RFID orientation recovery. RF-Reality represents the first successful marriage of the capabilities of all four. By taking advantage of previous work synthesizing an ultrawide bandwidth on commercial RFID tags for improved localization [45] and accelerating its performance, this thesis presents a system which makes the benefits of RF localization accessible for virtual and augmented reality systems like those currently on the market.

2.1   Ultrawideband (UWB) Tags

In the event that the line-of-sight between the reader and an RFID tag is obscured, the localization challenge takes on a new complexity. Generally, many RF localization strategies involve estimating the channel between the reader and the object of interest, like an RFID tag. The channel can be modeled as

$$H(f) = \sum_{i \in paths} A_i(f) \exp(j2\pi f \tau_i) \tag{2.1}$$

where f is the frequency of the signal, $A_i(f)$ is the channel amplitude (the inverse of channel attenuation along path i), $j = \sqrt{-1}$, and τ_i is the signal time of flight along path i (from which one can derive signal propagation distance along path i).

In sparse multipath environments, the channel is dominated by the direct line-of-sight path. Thus, performing an IFFT on the channel $H(f)$ will result in a time-domain function with a single magnitude peak at the signal time-of-flight. If we denote this time-of-flight $\tau = d \times c$ where d is the signal propagation distance and c is the signal propagation speed, the resolution with which we can determine the position of the object of interest d is

$$\delta_r = \frac{c}{2B} \tag{2.2}$$

where B is the signal bandwidth. It follows that, if there exists a second signal path

in addition to the line-of-sight path which has a length within $d \pm \delta_r$, then we would be unable to distinguish between the two paths by looking at the IFFT output.

One can improve position resolution by increasing the signal bandwidth B. However, off-the-shelf RFID's have a very limited communication bandwidth, corresponding to a position resolution of a few meters. Localization challenges like virtual reality need to be able to distinguish multipath much closer to the line-of-sight than this allows.

To overcome the standard communication bandwidth of commercial RFID tags being too small to enable accurate RFID localization, recent proposals have suggested creating new tags which can support a significantly larger bandwidth, then use that bandwidth to facilitate improved localization accuracy [15, 44, 57, 76]. While these techniques do improve localization accuracy and successfully disentangle multipath by increasing the bandwidth used to communicate with and locate the tag, such proposals exhibit a multitude of practical limitations:

- By requiring the development of new tags, such proposals effectively leave behind the billions of RFID tags currently in use throughout industry. Any large-scale adoption of this technology would require replacing the RFID tags currently in use with new equipment.

- These systems are comparatively costly. In contrast, because current off-the-shelf RFIDs are so ubiquitous, they benefit from economies of scale, reducing their cost to 5 cents per tag.

- The Federal Communications Commission (FCC) in the US, as well as various other regulatory bodies throughout the world, places strict limitations on powerful wireless signal transmissions. Proposals which rely on ultrawideband communication are limited by law in the US to the ISM band [11], a 26 MHz band from 902-928 MHz. The utilization of the entire ISM band for localization would result in a measurement resolution of greater than five meters, far worse than that required to track fine body movement. Devices which achieve greater resolution by increasing the bandwidth require hardware modifications, leaving out the billions of tags already produced and deployed.

- RFID communication is currently governed by the EPC Gen2 protocol [1]. The UWB tags proposed do not yet comply fully with the EPC Gen2 protocol and thus do not effectively communicate with commercial readers such as Thing-Magic [5] or Impinj [3].

RF-Reality overcomes these challenges by synthesizing an ultrawide bandwidth like the one demonstrated in RFind [45] instead of using a custom-built tag. Thus, RF-Reality can achieve the high localization resolution of UWB tags without the need to replace currently existing infrastructure, incurring their cost, violating FCC regulations, or disrupting the EPC Gen2 protocol.

2.2 Virtual and Augmented Reality (VR/AR) Systems

Today's virtual and augmented reality (VR/AR) systems almost all rely on vision-based techniques. Those that do can be broadly classified into two categories: hand- and headset-based devices and centralized tracking point-based motion capture systems.

The former category consists of devices such as Facebook's Occulus Rift [54] and Sony's PlayStation VR [65]. These devices require the user to carry the VR/AR system with them as they move, allowing a mobile headset to track the relative motion of the world around them visually. The latter category includes systems like the VICON [9] and OptiTrack [8] motion capture systems which instead track general motion via small optical markers (e.g. reflective spheres) placed on the user. RF-Reality is most similar to this second class because it uses small RFID stickers to track general motion similar to the optically localized markers used by VICON and OptiTrack.

Other non-vision-based VR/AR sensors that have been proposed include the inertial [58, 73], acoustic [67], magnetic [17], and mechanical [51]. While such systems overcome some of the drawbacks of vision-based techniques, they all require the user to carry tracking objects that are more expensive than RFID's and also require batteries or external power supplies that RFID's do not.

2.3 Radio Frequency (RF) Localization

RF localization has been well studied for over a century [28]. Shortly after the invention of RFID technology, research began to adapt and apply these techniques to localization of passive and active stickers. Beyond simply being able to determine whether or not an RFID was in range of a reader, early attempts at more quantitative localization used the strength of the signal received after reflecting off the RFID to estimate its distance to the reader [19, 21, 53, 78]. Other methods that incorporated the measured phase of the received signal could be used to track the relative motion of tags [40, 16]. Further methods combined measurements across multiple antennas in an array to more accurately estimate the angle of arrival (AoA) of a received signal [18, 77, 37, 46]. However, none of these early methods can handle multipath caused by the signal reflecting off objects in the environment (i.e. they have an inherent *line-of-sight* assumption).

Many state-of-the-art proposals have developed methods of improving localization accuracy and resolving multipath. These techniques can be broadly classified into four categories:

- **Dense Infrastructure.** By densely outfitting the localization space with reference tags, these techniques [20, 23, 69] can map received signal data to known position markers located *a priori*. Despite their high accuracy and low latency,

these techniques do not scale well as they are highly dependent upon a large number of reference tags placed throughout the entire localization space.

- **Motion-Based.** Similar to a RADAR using the movement of the tracked object (or the antenna itself) to localize accurately, many state-of-the-art techniques [52, 69, 75] rely on exact motion to locate objects of interest. However, such methods require either *a priori* knowledge of tag trajectory and speed or several seconds for a single measurement while the reader moves and gathers data.

- **Location Tracking.** Another set of techniques can determine the relative motion of RFID tags with very high precision by continuously calculating and unwrapping received signal phase [70, 74, 61, 32]. While such methods can estimate *changes in position* both accurately and quickly, initial position estimates can be off by tens of centimeters. Because the strength of these techniques comes from their ability to follow changes in position rather than the absolute location of the RFID, such initial estimation errors propagate throughout the experiment.

- **Frequency Hopping.** The most accurate absolute localization methods step through a large bandwidth of sensing frequencies, then combine across measurements to estimate a single *time-of-flight* (TOF) for signals reflecting off a static RFID [40, 45]. Unfortunately, in order to achieve sub-centimeter accuracy, these systems need to step over hundreds of megahertz of bandwidth and take several seconds to compute a single location estimate.

RF-Reality combines the low latency of location tracking techniques with the sub-centimeter accuracy of frequency hopping by transmitting the entire sensing bandwidth simultaneously. RF-Reality builds on RFind [45], which introduced the concept of two-frequency excitation for decoupling sensing from communication. However, whereas RFind transmits each frequency in its own time window, RF-Reality estimates the entire wideband channel in one shot. Thus, it can compute a new, accurate, absolute location estimate independent of all previous measurements dozens of times every second.

2.4 RFID Orientation

There are two challenges related to RFID orientation. First, even if a system does not need to extract an RFID's orientation in order to accomplish its task, the RFID's orientation still affects the channel. If the reader is equipped with a linearly polarized antenna, the channel's amplitude becomes a function of RFID orientation [61] meaning that a misaligned tag may not even be detectable [45, 70]. Replacing the linearly polarized antenna with a circularly polarized patch antenna allows for better detection ability, but the channel phase becomes a function of RFID orientation, complicating the localization challenge. The second challenge related to RFID orientation is how to use RF to sense tag orientation in addition to its location. Solutions to these challenges can be generally divided into four categories:

- **Received Signal Strength (RSSI)** approaches [48, 47, 61] rely on the coupling of channel amplitude and RFID orientation, particularly when using a linearly polarized antenna at the reader. In sparse multipath environments, channel amplitude for an RFID at a given orientation will remain relatively constant. However, when the tag begins to rotate, the RSSI of the RFID response will decrease as the RFID's antenna becomes further misaligned from that of the reader. Some techniques take advantage of this phenomenon along with other localization strategies such as phase tracking to recover both tag orientation and position [61] while others remove the effect altogether by normalizing by the minimum power required to energize the RFID [48, 47]. All of these methods, however, carry the critical line-of-sight assumption of RSSI-based localization techniques. In more multipath-rich environments, RSSI cannot guarantee accurate results.

- **Constrained Multi-Tag** techniques [68, 62, 24, 26, 72, 34, 12, 33, 14, 35] attempt instead to localize groups of similarly oriented RFID antennas and use the combined results to deduce individual tag orientations. For example, consider two RFID tags placed with equal orientations on the endpoints of a rigid beam of known dimensions. Even if the tag orientations are not known *a priori*, knowing that they are both oriented in the same direction would allow a localization scheme to calculate their relative positions. Because the dimensions of the beam are known, such approaches can use geometry to calculate the exact orientation of the tags. These techniques achieve high performance, even obtaining degree-level accuracy [68], but require multiple RFID's to be placed on a single rigid body in a known manner in order to accurately localize.

- **Dual-Antenna** methods [77, 42] leverage the constant effect of RFID orientation on received signal phase on coplanar receive antennas. By dividing the channel estimates from coplanar receive antennas, the orientation effect is eliminated, allowing for orientation-independent localization. RF-Reality extends this technique across multiple dimensions and with a larger localization bandwidth to decouple the phase effects of tag location and orientation.

- **Orientation Recovery** has been explored by some past work [25, 36, 59]. However, the proposed methods are intrinsically incapable of dealing with multipath. In addition, most of the experiments focused on recovering orientation while *fixing the location* of the tag. In contrast, RF-Reality incorporates mechanisms that allow it to recover orientation independent of location and in the presence of multipath.

RF-Reality accomplishes the orientation-extraction accuracy of multi-tag techniques with individual tags by leveraging the dual antenna approach across multiple dimensions to compute tag position. Then, we apply a fundamental physical understanding of how orientation affects phase to obtain robust, accurate estimates of both location and orientation.

Chapter 3

Speed Solution

3.1 Overview

The first challenge that must be overcome to use the great advantages of RF localization in VR/AR systems is latency. Recall that, while users require a latency of no more than 20 ms to avoid motion sickness [39, 50, 56], the most accurate absolute localization techniques require several seconds to take a single reading [45]. To solve this problem, RF-Reality leverages Orthogonal Frequency Division Multiplexing (OFDM) to compress the amount of time required to transmit the full frequency bandwidth.
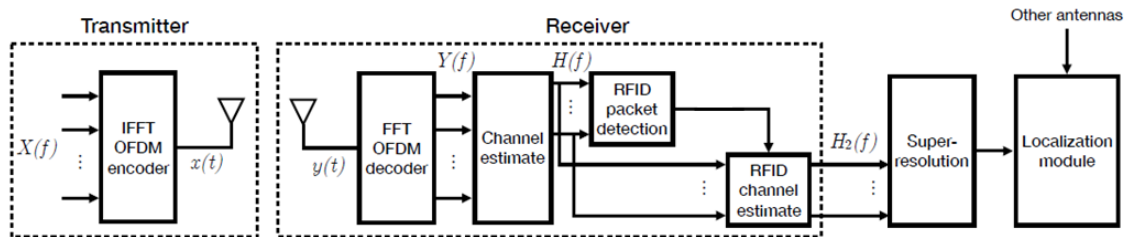

Figure 3-1: **Block Diagram of System Overview.**

A block diagram describing RF-Reality's speed solution is shown in Figure 31. First, a message encoded as a frequency-domain signal $X(f)$ is passed through an IFFT and transmitted as time-domain signal $x(t)$. After propagating through the environment and interacting with the RFID, the signal is received as $y(t)$ by a receiver and undergoes an FFT to become $Y(f)$. Because $X(f)$ and $Y(f)$ are both known, RF-Reality can estimate the channel $H(f)$. After a packet detection algorithm identifies the RFID reflection in the signal, the RFID channel $H_2(f)$ is computed. Having characterized the channel from the transmitter to the RFID to the receiver, RF-Reality uses a Super-Resolution algorithm to extract the time-of-flight. Finally, RF-Reality stitches the estimates from all receiving antennas to produce an absolute location estimate for the RFID.

23

3.2   OFDM Backscatter

3.2.1   Background

In general, RFID readers receive information from tags via backscatter communication. In backscatter networks, the reader acts as master to all other nodes, delivering power and scheduling all communication. The reader does this by first transmitting a single continuous wave to deliver power to nearby devices. Then, to communicate, the reader modulates the broadcast signal using one of three amplitude shift keying (ASK) modes: single-sideband (SSB), double-sideband (DSB), or phase reversal (PR) using a pulse-interval encoding (PIE) format [1]. Because the same RF carrier is used to deliver power as well as to communicate, all RFID's close enough to receive their operating energy from the reader's transmission also receive the broadcast message. After transmitting the message, the reader continues delivering power via continuous wave transmission.

When the reader first begins transmitting, nearby RFID's capture the energy via antennas and "power up." By sensing changes in power delivery, the tags decode the modulated instruction and respond accordingly. Because individual tags are unable to communicate with each other, the EPC Gen2 protocol has mechanisms that enable the reader to schedule access to the medium and prevent collisions. RF-Reality does work with multiple tags, but for now we will discuss the specific scenario where the reader communicates with a single tag.

To communicate with the reader, RFID tags take advantage of the reader's continuous wave transmission. In the default state, the tag's antenna harvests power from the transmitted signal. However, to communicate, the tag can change its state to reflect the signal received by its antenna instead of harvesting it. Thus, a reflected signal can be modulated by the RFID using either amplitude or phase shift keying (PSK) and encoded using either FM0 or Miller. This reflection can then be observed by the reader as a subtle change in the channel. By tracking the channel over time, an RFID reader can "see" the tag modulating its antenna impedance between reflective and non-reflective and decode the message from the RFID tag as an array of binary values.

Let us denote the signal transmitted by the reader as $x(t)$ and the signal received by the reader as $y(t)$. Assuming a narrowband channel, the received signal can be expressed as:

$$y(t) = \big(h_1 + h_2 \Gamma_{RFID}(t)\big)x(t) \tag{3.1}$$

where h_1 represents the channel when the RFID is not reflecting, h_2 represents the change in the channel from the additional signal paths created when the RFID is reflecting, and $\Gamma_{RFID}(t)$ represents the RFID's reflection coefficient, approximately either zero when the RFID is not reflecting or one when the RFID is reflecting.

Previous work [45] has leveraged this physical-layer channel effect to perform wideband stepped-frequency continuous wave (SFCW) localization. In commercial applications in the US, RFID communication bandwidth is typically limited to a maximum of 500 kHz from within the ISM band [1]. However, when the RFID is

powered by and receives instructions from a reader within the ISM band, its antenna will reflect signals across a large band of frequencies, not just those used for communication. Thus, **by combining this standard communication signal with an ultra-low-power carrier wave at a different frequency as shown in Figure 3-2, one can effectively decouple sensing from communication and expand the bandwidth available for localization by hundreds of MHz.**
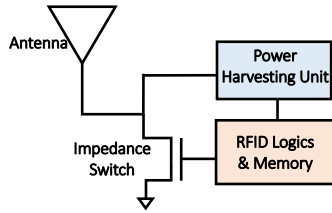
(a) RFID tag system diagram
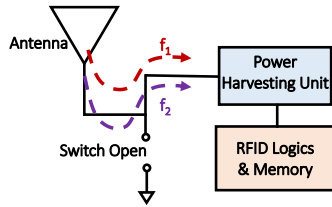
(b) Non-reflective state when antenna switch is "off"
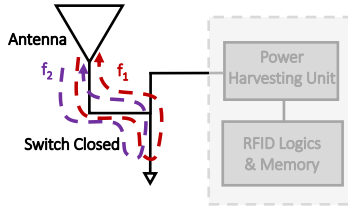
(c) Reflective state when antenna switch is on

Figure 3-2: **RFID Tag Antenna Impedance Control by Antenna Switch [45].** (a) RFID tag circuit diagram consisting of an antenna, antenna switch, power harvesting unit, and logic and memory circuitry. (b) RFID tag in non-reflective state. Antenna switch is turned "off," resulting in an open terminal. RF power flows into the power harvesting unit. (c) RFID tag in reflective state. Antenna switch is turned "on," resulting in a short terminal. RF power gets reflected by the ground.

This massive bandwidth expansion directly enables more accurate localization. Classically, SFCW resolution has been shown to improve with increasing bandwidth:

$$\delta_r = \frac{c}{2B} \tag{3.2}$$

where c represents the speed of light and B represents bandwidth. Furthermore, superresolution algorithms have been shown to further improve localization accuracy

results by an order of magnitude [45].[1] Historically however, when such methods have increased their bandwidth to the point at which they can achieve sub-centimeter localization, they require several seconds to perform the localization. Put simply, **a wider bandwidth increases both localization accuracy and measurement latency.**

3.2.2   Leveraging OFDM

Previously, because the sensing frequency was sequentially stepped across the entire bandwidth, a single measurement could take multiple seconds. This thesis leverages Orthogonal Frequency Division Multiplexing (OFDM) to drastically reduce the amount of time required to take a measurement. Specifically, OFDM is used in Wi-Fi and LTE communication to divide a large frequency band into independent subcarriers. Because of the independence of each narrowband subcarrier, the received OFDM signal $y(t)$ from Equation 3.1 can be transformed and rewritten in the frequency domain as:

$$Y(f) = \big(H_1(f) + H_2(f)\Gamma_{RFID}\big)X(f) \tag{3.3}$$

where $Y(f)$, $H_1(f)$, $H_2(f)$, and $X(f)$ are the frequency domain transformations of $y(t)$, $h_1(t)$, $h_2(t)$, and $x(t)$, respectively. $H_2(f)$, the component of the frequency-domain channel which contains only contributions from signal paths involving the RFID tag, can be fed through an IFFT and superresolution algorithm mentioned in Section 3.2.1. The resulting time-of-flight corresponds directly to the estimated position of the RFID via:

$$x = c \times TOF \tag{3.4}$$

where x is the round trip distance from the reader to the RFID and TOF is the output from the IFFT and superresolution, the time-of-flight.

To extract $H_2(f)$, we need to solve Equation 3.3. In reality, $X(f)$ is chosen by the reader and undergoes an IFFT before being transmitted as $x(t)$. The received signal $y(t)$ then undergoes an FFT to become $Y(f)$. Now that $X(f)$ and $Y(f)$ are known, the equation is re-arranged:

$$H(f) = \frac{Y(f)}{X(f)} = H_1(f) + H_2(f)\Gamma_{RFID} \approx \begin{cases} H_1(f) + H_2(f), & \text{if reflective} \\ H_1(f), & \text{if non-reflective} \end{cases} \tag{3.5}$$

When an RFID begins to respond to the reader's query, it first sends a preamble which is known to the reader. The reader can use this known preamble to isolate $H_1(f)$ when it knows the RFID is not reflecting, then subtract $H_1(f)$ from the observed channel $H(f) = H_1(f) + H_2(f)$ when it knows the RFID is reflecting to extract $H_2(f)$.

However, to ensure the entire channel $H_2(f)$ can be extracted, the RFID must

---

[1]For the purpose of this thesis, we do not need to delve into the details of how the IFFT or superresolution algorithms work. Rather, we can understand them as black boxes which take as input the component of the channel h_2 which is composed exclusively of RFID tag reflections and output the estimated time-of-flight.

remain in the reflective state for the duration of the OFDM symbol (i.e. the channel must be *slow-fading*). If it switches back to the non-reflective state before an OFDM symbol is completely reflected, any channel estimation algorithm would be unable to completely calculate $H_2(f)$ and, consequentially, no position estimate could be made. Thus, the following inequality must hold:

$$T_{symbol} < \frac{T_{switching}}{2} \tag{3.6}$$

where T_{symbol} is the duration of the OFDM symbol, given by:

$$T_{symbol} = \frac{N}{B} \tag{3.7}$$

where N is the number of subcarriers in the OFDM symbol and B is the total bandwidth of the OFDM symbol. $T_{switching}$, the period of time an RFID will remain in the reflective state while communicating with the reader, is given by:

$$T_{switching} = \frac{1}{BLF} \tag{3.8}$$

where BLF is the backscatter link frequency described in the EPC Gen2 protocol [1]. Equation 3.6 can therefore be rewritten:

$$N < \frac{B}{2BLF} \tag{3.9}$$

If Equation 3.9 holds, a channel estimation algorithm can calculate $H_2(f)$.

Finally, with $H_2(f)$ known, the IFFT and superresolution algorithms can be used to extract the time-of-flight and, critically, the position of the RFID tag.

To summarize, previous SFCW methods which emulated a wide bandwidth on off-the-shelf RFID tags were either inaccurate or slow. They had to choose between limiting their bandwidth and producing less accurate results more quickly, or stepping through a wider bandwidth one frequency at a time to produce more accurate results with a frame rate of less than one Hertz. By leveraging OFDM, this thesis collects an entire wideband channel in less time than it takes the RFID to respond, **eliminating the trade-off between localization accuracy and measurement latency**.

3.3 Implementation

We implement RF-Reality's speed solution using Ettus USRP X310's with UBX daughterboards and USRP N210's with SBX daughterboards [2] as shown in Figure 3-3. We use one USRP N210 with an SBX daughterboard to transmit power to the RFID tag and generate the query command [1] recognized by the RFID tag to initiate communication. For localization in three dimensions, we use two USRP X310's with two UBX daughterboards each (a single USRP X310 can support two simultaneous data streams). One UBX daughterboard is used to generate the repeated
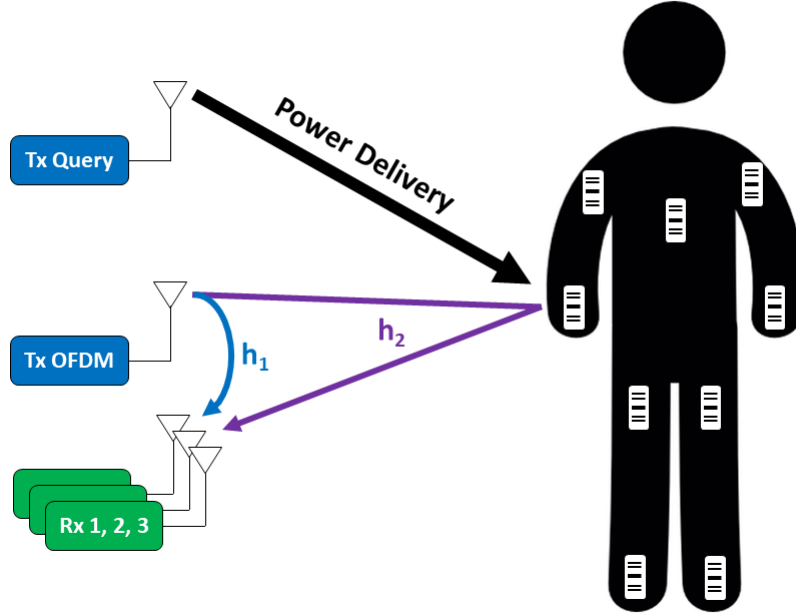
Figure 3-3: **Implementation of RF-Reality.** One USRP is used to deliver power and instructions to the RFID tags. A second USRP is used to transmit the OFDM symbols to the tag, which are then reflected and received by D USRP's, where D is the number of dimensions in which to localize.

OFDM signal used for wideband localization. The remaining three daughterboards are used as receivers. The USRP X310's can sustain up to 200 MSps and the UBX daughterboards have a bandwidth of 160 MHz. In our evaluation, the sampling rate is set to 100 MSps. All USRP X310's are synchronized with a OCTOCLOCK-G CDA-2990 8-Channel Clock Distribution Module [2].

Each daughterboard transmits or receives signals via MTI MT-242025 right-hand circularly polarized patch antennas [7] over Hand-Flex 086 Coaxial Cables [6]. Each receive antenna is separated from the transmit antennas by approximately 40 cm, and all are placed together on one side of the person being tracked.

All USRP X310's are connected over Ethernet to a high performance desktop PC running Ubuntu 17.04 with an 8-core 64-bit Intel Corei7 processor and 16 GB of RAM. To support high data rates, we use the Intel Converged Network Adapter X520-DA2 [4].

The algorithm described in Section 3.2.2 is implemented in the USRP UHD driver in C++ and runs in real-time. The OFDM symbols use $N = 20$ subcarriers over $B = 100$MHz of bandwidth and the backscatter link frequency is set to $BLF = 40$kHz to ensure more than one OFDM symbol can be reflected by the RFID in accordance with Equation 3.9. Each receive stream undergoes an FFT, packet detection, channel estimation, IFFT, superresolution, and time-of-flight estimation to output a new position estimate. At this point, every position estimation is algorithmically independent from all prior estimates, but in our implementation, we smooth the results using a Kalman filter.

Simultaneously, a different computer is connected to the USRP N210 with SBX daughterboard. This USRP acts as an RFID reader, delivering power to and initiating communication with the RFID. For the purposes of this thesis, we did not need to implement the entire EPC Gen2 protocol. To instruct the RFID to respond so the system can perform channel estimation, we only need to transmit the Select and Query commands [1] and then allow time for the RFID to respond with an RN16. The Select and Query commands instruct specific tags to respond (or not respond) and set important parameters such as the backscatter link frequency (BLF), which determines $T_{switching}$ as shown in Equation 3.8.

We used Alien Squiggle [13] RFID tags in our implementation of RF-Reality. Alien Squiggle tags are commercially available, off-the-shelf, passive UHF RFID tags which cost between 5-10 cents per tag.

3.4   Results

To realize RF-Reality as a solution for VR/AR systems, it must both match the sub-centimeter localization accuracy of previous work in wideband SFCW localization while achieving sub-twenty millisecond latency to avoid user motion sickness. Throughout the evaluation, it is useful to compare RF-Reality's performance to those of RFind [45], the state-of-the-art in accurate absolute RFID localization, and RF-IDraw [70], the state-of-the-art in low-latency RFID tracking.

To measure the ground truth for each of these measurements, we used an OptiTrack optical tracking system. The system is comprised of four cameras mounted on tripods approximately two meters in the air completely surrounding the localization environment. The cameras track small, spherical markers which reflect infrared light. By placing these markers next to the RFID tags, we can capture the ground truth locations of the tags for comparison with the system output. For non-line-of-sight testing, we only occlude the line-of-sight between the RFID tags and the USRP antennas; the view of the OptiTrack cameras remains unobstructed.

We evaluated RF-Reality in a standard office building. The evaluation environment is fully furnished with tables, chairs, computers. We evaluate RF-Reality in both line-of-sight and non-line-of-sight settings and perform a variety of single-tag and multi-tag tracking experiments. We perform NLOS testing similar to past work [45, 70] by blocking the visible LOS path between an RFID and RF-Reality's antenna using wooden dividers.

3.4.1   Localization Accuracy

We begin by comparing the localization accuracy of RF-Reality to state-of-the-art techniques RFind and RF-IDraw. For this evaluation, we limit our localization space to two dimensions in fairness to RF-IDraw, which has only demonstrated 2D RFID position tracking, and perform the test without tag motion in fairness to RFind, which takes several seconds to localize.
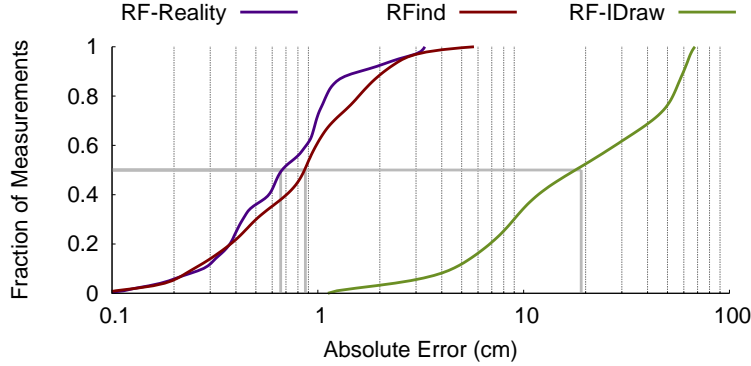
Figure 3-4: **Comparison to State-of-the-Art Baselines.** We show the CDF of 2D localization accuracy for RF-Reality (violet), RFind (red), and RF-IDraw (green).

We performed over 400 experimental trials in total with RF-Reality, RFind, and RF-IDraw, each time varying the RFID's location in our evaluation region. Figure 3-4 plots the CDFs of the 2D localization accuracy for the three systems. The figure reveals the following findings:

- In static settings, RF-Reality's accuracy closely matches that of RFind, both achieving sub-centimeter 2D localization accuracy and a 90th percentile error smaller than 3 cm. In principle, this is expected since both techniques can estimate a large bandwidth on off-the-shelf RFID's.

- Both RF-Reality and RFind outperform RF-IDraw, which has a median accuracy of 19 cm. This result is also expected since RF-IDraw is designed for high tracking accuracy rather than very high localization accuracy. In the RF-IDraw paper [70], the authors call this the initial position error.

- Finally, we note that, even though RFind has larger overall bandwidth than RF-Reality (around 200 MHz vs RF-Reality's 100 MHz), we believe the reason why RF-Reality can still match RFind's accuracy is due to the Kalman filter which is enabled by its very high frame rate. It is also important to note that while our current implementation uses only 100 MHz of bandwidth, this limitation is primarily imposed by the USRP X310 and our processing time. In practice, RF-Reality's approach is more general and can apply to any localization OFDM bandwidth.

We also plot RF-Reality's 3D localization accuracy in line-of-sight and non-line-of-sight environments in Figures 3-5 and 3-6, respectively. We collect 50,000 location measurements from our experimental trials. In these trials, we place an RFID tag inside of our evaluation space and perform a variety of 3D gestures at a natural pace to emulate the potential use of RF-Reality in a commercial application such as a VR/AR tracking system. In NLOS settings, we ensure that the visual LOS path is blocked from all of RF-Reality's antennas by wooden dividers.

Figures 3-5 and 3-6 plot the CDFs of the location errors in each of the x, y, and z dimensions for both LOS and NLOS settings. We make the following observations:
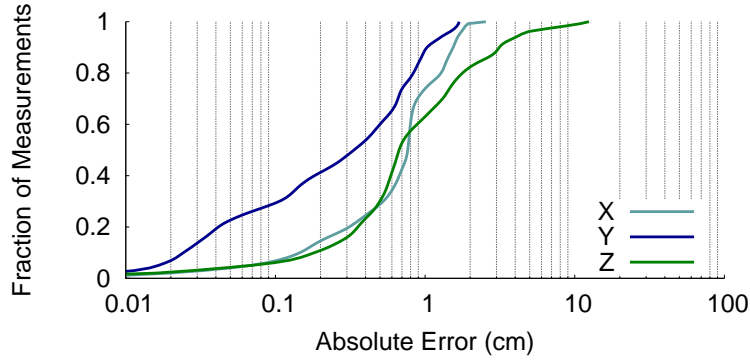
Figure 3-5: **CDF of 3D Localization Accuracy in Line-of-Sight.** RF-Reality's localization error in LOS along each of the x/y/z dimensions.
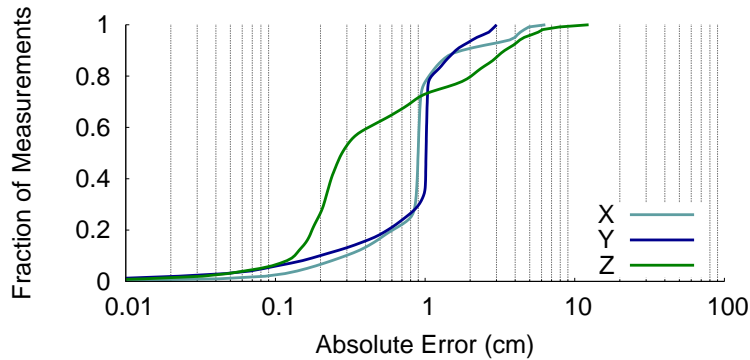

Figure 3-6: **CDF of 3D Localization Accuracy in Non-Line-of-Sight.** RF-Reality's localization error in NLOS along each of the x/y/z dimensions.

- RF-Reality meets the accuracy requirement for VR tracking in both LOS and NLOS settings. Specifically, it achieves a median error around or less than 1 cm along each dimension. Moreover, even its 90th percentile error is less than 2 cm in x/y and less than 3 cm in the z dimension.

- The accuracy in LOS is slightly better than its accuracy in NLOS settings. This is expected since the SNR of the line-of-sight path degrades in NLOS, resulting in lower accuracy.

3.4.2   Latency, Frame Rate, and Speed

In order to prove RF-Reality's utility as a VR/AR system, it must be able to produce accurate location estimates with a latency of less than 20 milliseconds to avoid inflicting the user with VR sickness. This translates to a minimum frame rate of 50 Hz. Additionally, RF-Reality must be able to accurately track motion in real-time.

   Figure 3-7 plots the CDF of RF-Reality's 2D and 3D localization latency for a single RFID. The latency is computed as the time difference between the time the USRP obtains an RFID response and the time it outputs a location. Note that
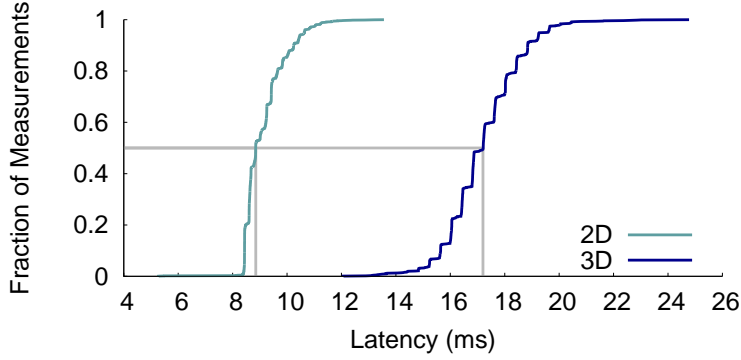
Figure 3-7: **RF-Reality's Latency.** We plot the CDF of the localization latency for 2D and 3D localization/tracking.
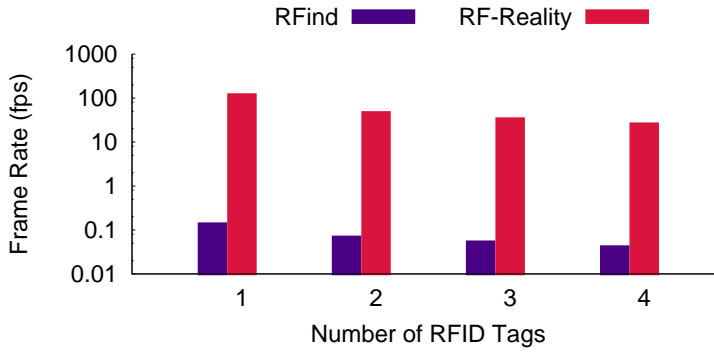
Figure 3-8: **Frame Rate.** We compare RF-Reality's frame rate when tracking 1-4 RFID's to that of RFind.

we ignore the time-of-flight of the wireless signal since it is only few nanoseconds for the distances of testing (few meters), and hence it is negligible for our latency measurements.

Figure 3-8 plots the frame rate of RF-Reality against the state-of-the-art technique, RFind. The frame rates are plotted with respect to various numbers of tracked tags.

We make the following observations from the figures:

- RF-Reality meets the latency requirement for VR/AR tracking. Specifically, both the median and 90th percentile latency measurements for 2D and 3D tracking are less than the 20 ms threshold. Specifically, the median latency for 2D and 3D tracking is 8.9 and 17 ms, respectively, and the 90th percentile latencies are 10 and 19 ms, respectively.

- Our latency is primarily limited by the processing time of the computer rather than the latency of the RFID's response or acquisition. Specifically, in both the 2D and 3D experiments, our receivers all obtain the RFID responses at the same time, yet the difference in latency is due to the difference in processing speed. Indeed, RF-Reality's 3D latency is more than twice its 2D latency due

32

to limited computational resources.

- The figure shows that the latency CDF's are discretized. This is because when our localization algorithm is using all the processor's computational resources, it drops entire buffer-lengths of RFID packets.

- RF-Reality drastically outperforms the state-of-the-art in accurate absolute RFID localization when comparing frame rates. Because today's off-the-shelf readers can query hundreds of tags per second, by further optimizing our implementation of RF-Reality or using more powerful processors, we can easily scale to a larger frame rate and lower latency.

- After one tracked RFID tag, there is a roughly linear decline in the maximum achievable frame rate. This is because RF-Reality, like other state-of-the-art techniques, only localizes one tag per measurement.
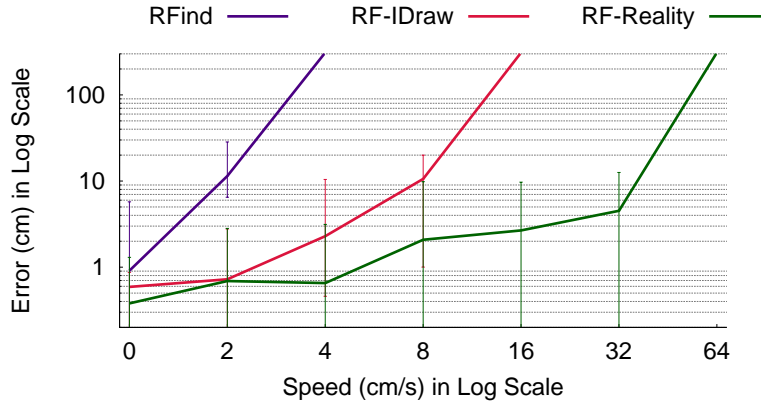
Figure 3-9: **Tracking Error vs. Speed of Motion.** We compare the 2D tracking accuracies of RF-Reality (green), RF-IDraw (red), and RFind (violet).

We would also like to compare RF-Reality's localization tracking accuracy to state-of-the-art techniques RFind and RF-IDraw. In fairness to RF-IDraw, we focus on 2D tracking since RF-IDraw is evaluated in 2D. We perform 40 experimental trials, each time varying the speed at which an RFID moves. Figure 3-9 plots the median tracking accuracies of RFind, RF-IDraw, and RF-Reality. It is important to note that the figure is in log-log scale to demonstrate how much RF-Reality is more capable in maintaining its accuracy despite high speed motion.

We make the following observations:

- RFind has the earliest point of failure. Its error increases to over 10 cm when the RFID moves faster than 2 cm/s and completely fails at 4 cm/s. This result is expected because RFind's frequency hopping is a time consuming process, requiring several seconds for channel acquisition alone. Hence, its mathematical assumption that the object being localized be static fails and leads to high errors even at low speeds.

- RF-IDraw performs better than RFind in terms of tracking. Note that in this result, we eliminate the initial position error as per RF-IDraw's implementation. Still, it incurs over 10 cm of error for speeds larger than 8 cm/second. Beyond these speeds, RF-IDraw's ability to track and unwrap the received phase decreases in the presence of noise.

- Finally, RF-Reality outperforms both RF-IDraw and RFind and sustains centimeter-scale accuracy even at speeds of 16 cm/s and sub-10 centimeter errors at speeds of 32 cm/s. This is due to two reasons: first is its significantly higher frame rate and single-shot bandwidth acquisition in comparison to RFind. And second, due to its large bandwidth, it has more resilience to frequency selective fading than RF-IDraw.

Chapter 4

Orientation Independence

The second challenge that must be overcome to use the great advantages of RF localization in VR/AR systems is the effect of orientation on location estimation. Recall that current RFID localization systems can only achieve accurate results if the tag's orientation remains constant with respect to the reader. To enable orientation-independent RFID localization, RF-Reality uses one additional antenna per dimension to automatically remove the effect of orientation from channel phase and achieve accurate position estimates in real-world tracking scenarios.

4.1 Antenna Projection Symmetry

4.1.1 Polarization Primer

For a full primer on antenna polarization, I recommend Staelin, et al[66]. When a reader transmits power and instructions to the RFID, the signal propagates as an electromagnetic field. Assume the simple model of an antenna as a dipole. As alternating current excites the dipole, the electric field around it begins to vary as illustrated in Figure 4-1. As the current in the antenna oscillates, the resulting electric field in the region begins to change. The changing field propagates outward to eventually become incident upon the RFID's antenna.

If the RFID's antenna is oriented parallel to that of the reader (i.e. induced current in the RFID's antenna is allowed to flow in the same direction as that in the reader's antenna), then the RFID can harvest the energy of the changing electric field and respond accordingly. This can be visualized by placing a second charge carrier at the right hand side of Figure 4-1 free to oscillate along the vertical axis. Because its motion along the vertical axis is unconstrained, its motion would follow the yellow sinusoid as the electromagnetic wave continues to propagate toward it from the left. However, if the RFID's antenna is oriented perpendicular to that of the reader, that would be akin to constraining the motion of the second charge carrier along the dimension into and out of the page. In the far field, the electric field along this dimension is effectively constant. Thus, the charge carrier would remain motionless, no current would be generated, and the RFID would not be able to harvest any power with which to respond.

Direction of Current Flow in Antenna

Oscillating Charge Carrier

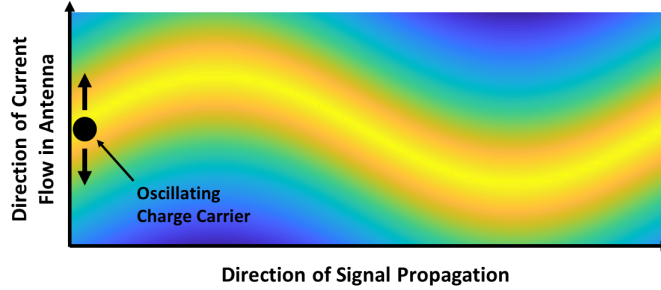**Direction of Signal Propagation**

Figure 4-1: **Electric Field Strength around an Antenna.** Color corresponds to the strength of the electric field at that point with yellow indicating a high magnitude and blue indicating a low magnitude. To envision the 3D electric field, revolve the field about the axis of oscillation along which the charge carrier moves.

In real world applications, this is problematic because any readers equipped with antennas that only allow current to flow along one axis (called *linearly polarized* antennas) are incapable of communicating with RFID tags with misaligned antennas. If RF-Reality could only track tags whose antennas were perfectly aligned with the reader, it would miss many real world body tracking scenarios where natural movement necessitates, for example, limb rotation.

To solve this problem, most readers today do not use linearly polarized antennas. Instead, they are equipped with circularly polarized antennas. Instead of generating a signal along a single electromagnetic plane wave, circularly polarized antennas can be thought of as two perpendicular linearly polarized antennas transmitting the same signal but with a 90 degrees phase difference between them. As illustrated in Figure 4-2, using a circularly polarized antenna almost eliminates problematic RFID tag antenna orientations.

E_y polarized electric field

When tag rotates by Φ the received phase changes by $\theta(\Phi)$
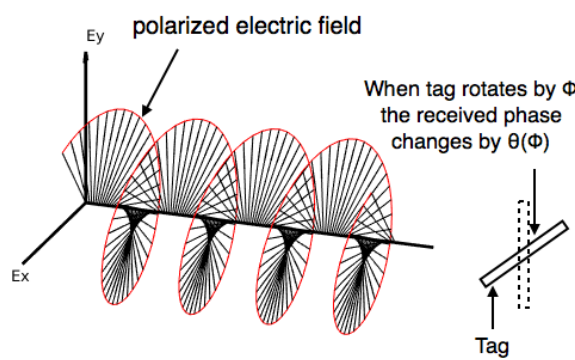
E_x

Tag

Figure 4-2: **Signal Propagation from a Circularly Polarized Antenna.** Because the electromagnetic wave measured at the RFID antenna is now oscillatory along two spatial dimensions instead of one, the tag can harvest power and respond regardless of how it is oriented.[2]

---

[2]Technically, the RFID tag antenna can not be oriented along the E_z dimension.

However, there is one large drawback to using a circularly polarized antenna: the phase of the reflected signal will vary with the tag's orientation as illustrated in Figure 4-2. Let the frequency domain signal reflected off a vertically oriented tag and received by the reader be denoted $Y(f)$ as in Equation 3.3. Even assuming no multipath, the frequency domain signal reflected off a tag and received by the reader would undergo a phase rotation to be $Y(f)e^{j\phi_o(\theta)}$ where $\phi_o(\theta)$ is the phase delay caused by orientation difference θ. This phase rotation will propagate through the channel estimation, IFFT, and SuperResolution algorithms, resulting in an erroneous position estimate. Simply put, translation of the RFID along the line of sight is indistinguishable from rotation about the line of sight. We solve this problem by leveraging the fact that the RFID's orientation will affect the received signals at nearby antennas similarly.

4.1.2   Orientation Cancellation

Recall from Section 3.2.2 how we estimate the channel state information (CSI) of signal paths involving the RFID tag, $H_2(f)$. Each narrowband component of the channel can be expressed as a complex number:

$$H(f) = A(f) \exp\big(j\phi(f)\big) \tag{4.1}$$

where $A(f)$ is the channel amplitude, $j = \sqrt{-1}$, and $\phi(f)$ is channel phase.

Two factors influence channel phase: the time-of-flight of the signal and the relative polarizations of the transmit, reflect, and receive antennas. Thus, the channel phase can be decomposed as follows:

$$\begin{aligned} \phi(f) &= \phi_0(f) + 2\pi f \tau + \phi_o(\theta) \\ &= \phi_0(f) + 2\pi \frac{d}{\lambda} + \phi_o(\theta) \end{aligned} \tag{4.2}$$

where $\phi_0(f)$ is the initial phase offset due to the transmission delay of the signal through the hardware, f is the center frequency of the channel H, τ is the time-of-flight of the signal $\tau = c \times d$ where c is the speed of light and d is the signal propagation distance from the transmitter to the reflector to the receiver, λ is the signal wavelength, and $\phi_o(\theta)$ is the phase contribution from the relative antenna orientation θ. For now, it is not necessary to characterize $\phi_o(\theta)$; rather it is sufficient to say that it contributes to channel phase independently of the signal time-of-flight.

After transmitting the frequency domain signal $X(f)$ and receiving $Y(f)$, Equation 3.5 describes how we isolate and calculate the channel state information of signal paths involving reflections off the RFID tag, $H_2(f)$. As always, we remove the phase delay of the hardware by calibrating to a reference point at a known distance d_{cal}. If we denote the calibrated channel estimate from receiver i to be $H^i(f)$, then it follows that:

$$H^i(f) = \frac{H^i_{2,new}(f)}{H^i_{2,cal}(f)} = A^i(f) \exp\Big(j\big(2\pi \frac{d^i_{new} - d^i_{cal}}{\lambda} + \phi^i_o(\theta^i_{new}) - \phi^i_o(\theta^i_{cal})\big)\Big) \tag{4.3}$$

where $H_{2,new}^i(f)$ is the RFID channel estimate from a new RFID location received at antenna i, $H_{2,cal}^i(f)$ is the RFID channel estimate from the calibration point received at antenna i, d_{new}^i is the signal propagation distance from the transmitter to the RFID at the new position to antenna i, d_{cal}^i is the signal propagation distance from the transmitter to the calibration point to antenna i, $\phi_o^i(\theta)$ is the phase difference caused by the relative orientation of the RFID to antenna i, θ_{new}^i is the relative orientation of the RFID at the new position to antenna i, and θ_{cal}^i is the relative calibration orientation of the RFID tag to antenna i.

To remove the effect of the relative orientation of the RFID tag to the receiver, we add a second identical receive antenna and position it such that its antenna plane is coplanar with the original receiver's antenna plane. If we denote the original antenna, antenna 1, and the second antenna, antenna 2, it follows that the quotient of the calibrated channel estimates of the two antennas can be calculated as:

$$H_{combined}(f) = \frac{H^2(f)}{H^1(f)} = \frac{A^2(f)}{A^1(f)} \exp\left(j\frac{2\pi}{\lambda}(d_{new}^2 - d_{new}^1 - d_{cal}^2 + d_{cal}^1)\right) \qquad (4.4)$$

Note that, because the two antennas have the same polarization, $\phi_o^1(\theta) = \phi_o^2(\theta)$. Furthermore, because the two antennas are placed such that they share a single antenna plane, their orientations relative to the RFID tag are identical, so $\theta_{new}^1 = \theta_{new}^2$ and $\theta_{cal}^1 = \theta_{cal}^2$. Thus, the effect of orientation on the combined channel $H_{combined}(f)$ is

$$\phi_o^2(\theta_{new}^2) - \phi_o^1(\theta_{new}^1) - \phi_o^2(\theta_{cal}^2) + \phi_o^1(\theta_{cal}^1) = 0 \qquad (4.5)$$

If we abstract the IFFT and Super-Resolution algorithms as a single function which takes as input a channel estimate and returns the distance:

$$\text{SR}[A(f)\exp(j2\pi\frac{d}{\lambda})] = d \qquad (4.6)$$

it follows that the difference in the signal propagation distance from the transmitter to the RFID to receiver 1 and that to receiver 2 can be calculated by:

$$d_{new}^2 - d_{new}^1 = \text{SR}[H_{combined}(f)] + d_{cal}^2 - d_{cal}^1 \qquad (4.7)$$

By combining this distance estimate with estimates from a second pair of receive antennas oriented perpendicularly to the first pair, one can solve the two equations to pinpoint the new RFID location in two dimensions. Adding a fifth antenna on a final orthogonal plane localizes the RFID in all three dimensions regardless of RFID orientation.

To summarize, **by combining channel estimates across two antennas in each dimension, we remove the dependence of RFID orientation on the channel** and extract accurate position estimates regardless of RFID orientation.

4.2 Implementation

We implemented RF-Reality's orientation dependence solution on Ettus USRP N210's with SBX and LFRX daughterboards [2]. We use one USRP equipped with an SBX daughterboard to transmit the query command and continuous wave. Over time, this USRP performs frequency hopping on the continuous wave to cover the entire bandwidth. For orientation-independent localization in one dimension, we use two receive USRP's, each with an LFRX daughterboard, placed approximately 40 cm to either side of the transmitting antenna.

In our evaluation, we stepped the transmission frequency over 200 MHz. All USRP's are synchronized with a OCTOCLOCK-G CDA-2990 8-Channel Clock Distribution Module [2]. Each USRP transmits or receives signals via MTI MT-242025 right-hand circularly polarized patch antennas [7] over Hand-Flex 086 Coaxial Cables [6].

The receive chains are designed to perform coherent decoding, similar to an off-the-shelf reader. Each consists of a filter, a variable gain low noise amplifier (LNA), and an I/Q mixer. The filter reduces noise and environmental interference. After filtering, the received signal is amplified by an LNA and down-converted to baseband by mixing with the sensing frequency through an I/Q mixer that feeds to an LFRX daughterboard of the USRP. The USRP's sample baseband I/Q signals which are postprocessed in MATLAB similar to [45].

One major difference exists in the MATLAB implementation of RF-Reality's orientation-independent localization algorithm: instead of solving for the intersection of ellipsoids, RF-Reality's *distance difference* calculation requires solving for the intersection of hyperboloids. Because of the geometric differences between the shapes, RFID positions further from the receivers are prone to higher localization error.

As before, we used Alien Squiggle [13] RFID tags in our implementation of RF-Reality.

4.3 Results

We focus on evaluating RF-Reality's orientation-independent localization in one dimension and compare the result to RFind. RFind uses the same wide bandwidth synthesis technique as RF-Reality but has no method of decoupling the effects of orientation and time-of-flight from the channel estimate. In this evaluation, we begin by randomly placing the RFID in the localization space on a measurement mat in front of the antennas, then randomly choose an orientation between 0 and 360 degrees using a paper protractor. We collect measurements using both RFind and RF-Reality and compare the results to the ground truth from the measurement mat. We plot the CDF of the measurement errors from 450 trials of both methods in Figure 4-3. The figure shows the following findings:

- RF-Reality maintains its very high localization accuracy despite orientation changes. Specifically, the median error remains sub-centimeter and the 90th
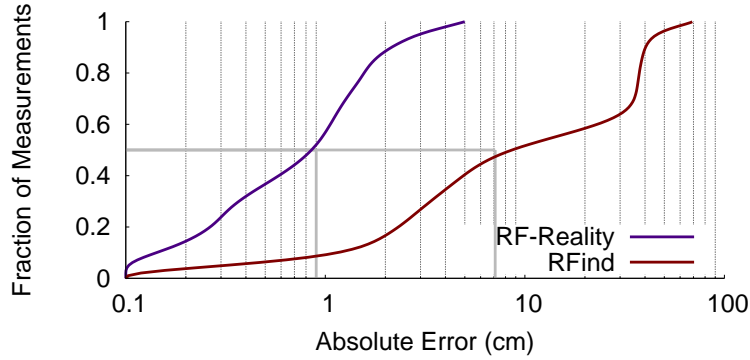
Figure 4-3: **Effect of Orientation on Localization Accuracy.** We plot the CDF of localization accuracy as we vary an RFID's orientation for both RF-Reality (violet) and RFind (crimson).

percentile error remains less than 3 cm. These errors demonstrate the impact of tag orientation is negligible on RF-Reality's accuracy.

- In contrast, RFind suffers from a significant degradation in its localization accuracy due to orientation. Specifically, its median error increases more than $8\times$ (from sub-centimeter to 8 cm).

These results demonstrate that RF-Reality is capable of accurately localizing an RFID regardless of tag orientation.

Chapter 5

Orientation Extraction

In addition to sensing the position of an object of interest, VR/AR systems also need to be able to extract object orientation. Many previous methods have accomplished this goal by placing several RFID's on known locations on the object and localizing each of them individually, then using their relative locations to reconstruct the object's orientation [68, 62, 24, 26, 72, 34]. In fact, many optical tracking systems such as VICON [9] and OptiTrack [8] extract object orientation similarly by requiring users to place three or more markers on each rigid body. This strategy can achieve a high level of accuracy, but requires highly constrained RFID tag placement. Furthermore, because latency scales with the number of tracked RFID's as shown in Figure 3-8, it is desirable to minimize the number of simultaneously tracked tags.

RF-Reality can sense the orientation of individual tags. Unlike previous single-tag techniques which rely on RSSI-based orientation extraction [61], RF-Reality leverages the phase-dependence of the channel using a circularly polarized antenna to calculate a tag's orientation. Because RF-Reality isolates the channel corresponding to paths involving the RFID tag, we will discuss that channel exclusively in this section.

5.1 Effect of Antenna Polarization on the Physical Channel

5.1.1 Signal Polarization and Propagation

As in Figure 4-2, assume the signal from a circularly polarized antenna propagates along the z dimension toward the RFID tag with a two-dimensional polarization in the x and y directions. The polarization of the wave can generally be described using a normalized polarization-plane vector [29]:

$$\hat{e} = \frac{\hat{x} + j\gamma\hat{y}}{\sqrt{1 + \gamma^2}} = \frac{1}{\sqrt{1 + \gamma^2}} \begin{bmatrix} 1 \\ j\gamma \end{bmatrix} \qquad (5.1)$$

where γ is the polarization constant and $\hat{x}$ and $\hat{y}$ are unit vectors in the x and y dimensions, respectively. If we label the polarization constant of the transmit and

receive antennas α and that of the RFID antenna β, then we have:

$$\hat{e}_{tx} = \hat{e}_{rx} = \frac{1}{\sqrt{1+\alpha^2}} \begin{bmatrix} 1 \\ j\alpha \end{bmatrix}$$

$$\hat{e}_{RFID} = \frac{1}{\sqrt{1+\beta^2}} \begin{bmatrix} \cos(\theta) & \sin(\theta) \\ -\sin(\theta) & \cos(\theta) \end{bmatrix} \begin{bmatrix} 1 \\ j\beta \end{bmatrix} \tag{5.2}$$

where $\hat{e}_{tx}$, $\hat{e}_{rx}$, and $\hat{e}_{RFID}$ are the polarization-plane vectors of the transmit, receive, and RFID antennas, respectively, and θ is the orientation of the RFID antenna relative to that of the transmit and receive antennas. Assume here that the transmit and receive antennas are oriented in the same direction and have equivalent polarizations. Figure 5-1 illustrates the effects of these polarizations as well as the signal propagation path itself on the physical channel.
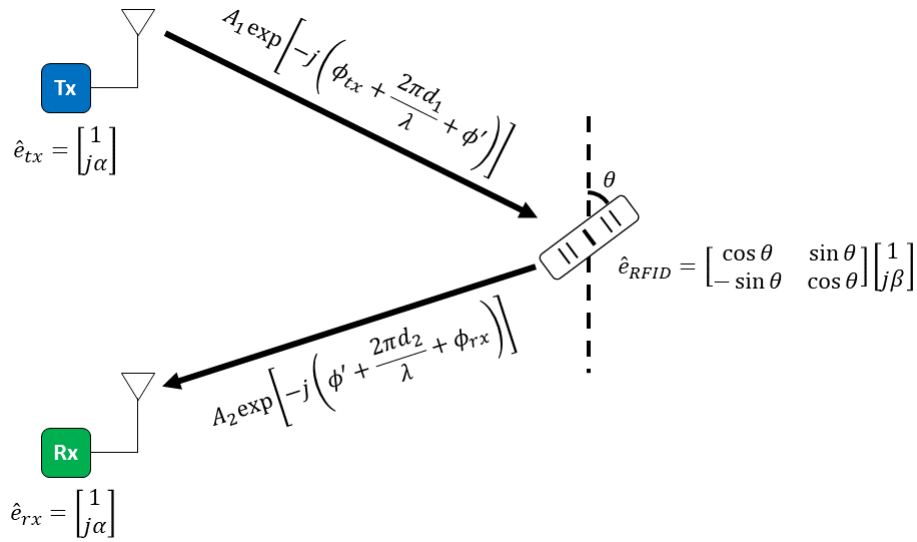

Figure 5-1: **Signal Polarization and Propagation.** As the signal is transmitted from the transmitter to the RFID to the receiver, its channel is affected by both the relative polarizations of the transmit, receive, and RFID antennas as well as signal propagation through the air. Note that θ describes tag orientation on the plane parallel to the antenna planes of the transmit and receive antennas.

As the signal x travels along the path from the transmitter to the RFID, it undergoes attenuation and phase delay, so the signal received at the RFID, v, is

$$v = A_1 \exp\big(-j(\phi_{tx} + \frac{2\pi d_1}{\lambda} + \phi')\big)x \tag{5.3}$$

where A_1 is the channel amplitude along the path from the transmitter to the RFID, ϕ_{tx} is the phase delay of the transmit antenna and hardware, d_1 is the distance from the transmit antenna to the RFID, λ is the signal wavelength, and ϕ' is the phase delay of the RFID antenna.

The complex signal component arising from the signal incidence upon the RFID

antenna, e_v, can be calculated from the inner product of the normalized polarization-plane vectors of the transmit and RFID antennas, respectively:

$$e_v = \hat{e}_{tx}^* \cdot \hat{e}_{RFID} = \frac{1}{\sqrt{(1+\alpha^2)(1+\beta^2)}} \begin{bmatrix} 1 & -j\alpha \end{bmatrix} \left(\begin{bmatrix} \cos(\theta) & \sin(\theta) \\ -\sin(\theta) & \cos(\theta) \end{bmatrix} \begin{bmatrix} 1 \\ j\beta \end{bmatrix} \right)$$
$$= \frac{(1+\alpha\beta)\cos(\theta) - j(\alpha+\beta)\sin(\theta)}{\sqrt{(1+\alpha^2)(1+\beta^2)}} \tag{5.4}$$

As the signal is reflected off the RFID and and travels to the receiver, the process is repeated. A signal v traveling along the path from the RFID to the receiver will undergo another amplitude and phase delay, so the received signal at the receiver w will be:

$$w = A_2 \exp\left(-j(\phi' + \frac{2\pi d_2}{\lambda} + \phi_{rx})\right)v \tag{5.5}$$

where A_2 is the channel amplitude along the path from the RFID to the receiver, d_2 is the distance from the RFID to the receive antenna, and ϕ_{rx} is the phase delay of the receive antenna and hardware.

As before, the complex signal component arising from the signal incidence upon the receive antenna, e_w, can be calculated from the inner product of the polarizations of the RFID and receive antennas, respectively:

$$e_w = \hat{e}_{RFID}^* \cdot \hat{e}_{rx} = \frac{1}{\sqrt{(1+\alpha^2)(1+\beta^2)}} \begin{bmatrix} 1 & -j\beta \end{bmatrix} \begin{bmatrix} \cos(\theta) & -\sin(\theta) \\ \sin(\theta) & \cos(\theta) \end{bmatrix} \begin{bmatrix} 1 \\ j\alpha \end{bmatrix}$$
$$= \frac{(1+\alpha\beta)\cos(\theta) - j(\alpha+\beta)\sin(\theta)}{\sqrt{(1+\alpha^2)(1+\beta^2)}} \tag{5.6}$$

Note from Equations 5.4 and 5.6 that $e_v = e_w$. This is to be expected since the transmit and receive antennas are considered to be identical. They can be represented in polar coordinates as:

$$e = A_{pol} \exp\left(j \tan^{-1}\left(-\kappa \tan(\theta)\right)\right), \kappa = \frac{\alpha+\beta}{1+\alpha\beta} \tag{5.7}$$

where A_{pol} is the effect of the antenna polarization differences on the channel. To calculate RFID orientation θ, we do not need to characterize A_{pol}. κ can be thought of as a ratio representing both antenna polarizations. Kline [31] evaluates this for the special case of $\alpha = \beta = 1$.

5.1.2 Isolating Orientation Effects

Note that the impact of the antenna polarizations manifests as a phase delay. The received signal y can therefore be represented by:

$$
\begin{aligned}
y &= e_v e_w w \\
&= A_{pol}^2 A_1 A_2 \exp\left(j\left(\phi_{tx} + 2\phi' + \phi_{rx} + \tfrac{2\pi(d_1+d_2)}{\lambda} + 2\tan^{\text{-}1}\left(-\kappa\tan(\theta) \right) \right) \right) x \\
&= \quad A \quad\;\; \exp\left(j\left(\quad\quad \phi_0 \quad\quad + \quad \tfrac{2\pi d}{\lambda} \quad + \quad\quad \phi_o(\theta) \quad\quad\;\; \right) \right) x
\end{aligned}
\tag{5.8}
$$

where $A = A_{pol}^2 A_1 A_2$ is the amplitude of the channel, $\phi_0 = \phi_{tx} + 2\phi' + \phi_{rx}$ is the initial phase offset due to the transmission delay of the signal through the hardware, $d = d_1 + d_2$ is the signal propagation distance from the transmitter to the reflector to the receiver, and $\phi_o(\theta)$ is the phase contribution from the relative antenna orientation θ:

$$
\phi_o(\theta) = 2\tan^{\text{-}1}\left(-\kappa\tan(\theta) \right)
\tag{5.9}
$$

We have now characterized the effect of relative antenna orientation on channel phase discussed in Section 4.1.2. Unfortunately, the antenna polarization constants of RFID antennas are typically unknown, so we must estimate κ ourselves.

5.1.3 Calibrating α and β

Section 4.1.2 outlines an algorithm to remove the effect of orientation from channel phase. We perform a similar technique to isolate it. Recall from Equation 4.3 that the ϕ_0 can be removed via calibration by dividing channel estimates from measurements taken at two positions. If the position of the RFID is kept constant such that $d_{new} = d_{cal}$ but the new orientation θ_{new} is varied, the channel H can be expressed as:

$$
\begin{aligned}
H &= A\exp\left(j\left(\phi_o(\theta_{new}) - \phi_o(\theta_{cal})\right) \right) \\
&= A\exp\left(j2\left(\tan^{\text{-}1}\left(-\kappa\tan(\theta_{new})\right) - \tan^{\text{-}1}\left(-\kappa\tan(\theta_{cal})\right) \right) \right)
\end{aligned}
\tag{5.10}
$$

If the antenna polarizations are not known *a priori*, we perform a curve fitting algorithm to estimate κ. After computing H using the channel estimation algorithm described in Section 3.2.2, we solve Equation 5.10 for the new RFID orientation:

$$
\theta_{new} = \tan^{\text{-}1}\left(-\frac{1}{\kappa}\tan\left(\frac{\angle H}{2} + \tan^{\text{-}1}\left(-\kappa\tan(\theta_{cal})\right) \right) \right)
\tag{5.11}
$$

for $d_{new} = d_{cal}$.

We take measurements across several RFID orientations without changing the RFID's position and use Equation 5.11 to compute least-squares estimates of κ using a curve fitting algorithm.

5.1.4 Estimating Position and Orientation Simultaneously

Now that κ is known and we have taken a calibration measurement with the RFID at a known position d_{cal} and orientation θ_{cal}, we move the RFID to an unknown position and orientation. Using the position estimation algorithm described in Section 4.1.2, we compute the new RFID position d_{new}. After d_{new} is known, we substitute it and d_{cal} into Equation 4.3 and substitute Equation 5.9 for $\phi_o(\theta_{new})$ and $\phi_o(\theta_{cal})$. Solving for θ_{new} yields:

$$\theta_{new} = \tan^{-1}\left(-\frac{1}{\kappa}\tan\left(\frac{\angle H}{2} - \pi\frac{d_{new}-d_{cal}}{\lambda} + \tan^{-1}\left(-\kappa\tan(\theta_{cal})\right)\right)\right) \qquad (5.12)$$

Having calibrated for κ, measured H, calculated d_{new}, and selected d_{cal} and θ_{cal}, RF-Reality can estimate the position and orientation of an RFID.

5.2 Implementation

5.2.1 Hardware and Software Overview

The hardware implementation of RF-Reality's orientation extraction solution is identical to that described in Section 4.2. The algorithm is also implemented in MATLAB and ran sequentially with RF-Reality's orientation-independent localization software.

5.2.2 Calibration

Before running experiments to estimate the location and orientation of an RFID, we begin by calibrating to compute κ, the polarization parameter of the RFID tag's antenna described in Section 5.1. To do this, the RFID's position is held constant and the channel is measured by a receive antenna while the RFID's orientation is varied from 0 to 360 degrees in increments of 10 degrees. The resulting measurements are of the form:

$$H[\theta_i] = A[\theta_i]\exp\left(j(\phi + \phi_o[\theta_i])\right) \qquad (5.13)$$

where A is the channel amplitude, $\phi = \phi_0 + 2\pi f\tau$ is the component of channel phase which is a function of the signal time-of-flight, and ϕ_o is the component of channel phase which is a function of RFID orientation θ_i described by Equation 5.9.

If we divide by the channel calculated at the first angle orientation θ_0, we can calculate a normalized channel:

$$H'[\theta_i] = \frac{H[\theta_i]}{H[\theta_0]} = \frac{A[\theta_i]}{A[\theta_0]}\exp\left(j(\phi_o[\theta_i] - \phi_o[\theta_0])\right) \qquad (5.14)$$

which has phase:

$$\begin{aligned} \angle H'[\theta_i] &= \phi_o[\theta_i] - \phi_o[\theta_0] \\ &= 2\tan^{-1}\left(-\kappa\tan(\theta_i + b)\right) + c \end{aligned} \qquad (5.15)$$
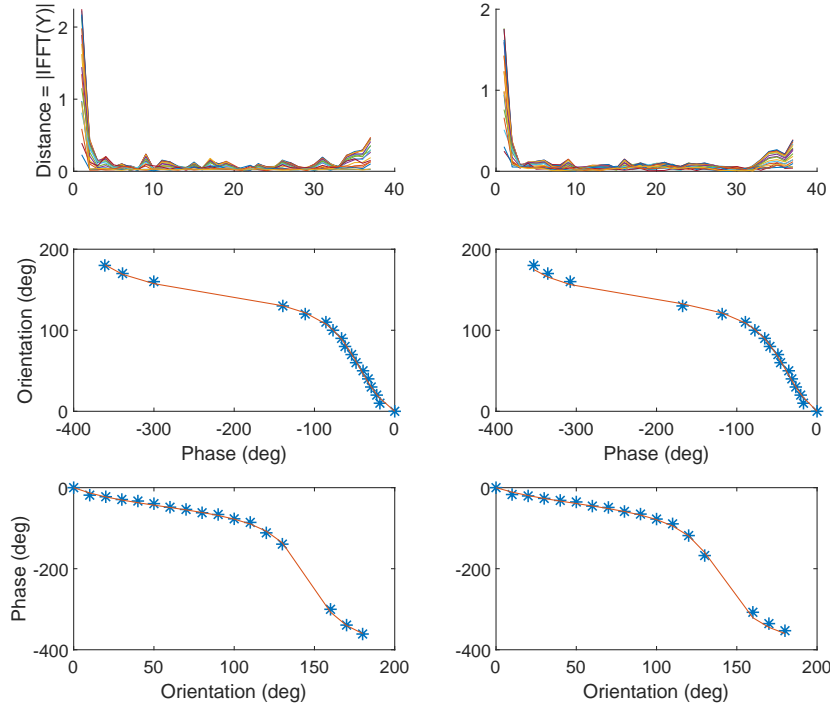
Figure 5-2: **Results of Curve-Fitting to Orientation-Phase Data.** Columns one and two represent the results from receive antennas one and two, respectively. Row one is the absolute value of the IFFT output for each carrier frequency vs. orientation. Row two is the orientation of the tag as a function of the unwrapped phase of the response with blue stars indicating collected data and the red line indicating the fit. Row three is the inverse relationship, unwrapped response phase vs. orientation of the tag.

where b is a parameter to account for the initial orientation offset[1] and $c = -\phi_o[\theta_0]$. Both are treated as a third parameter for the curve fitting algorithm.

We then perform a least-squares fit on the channels $H'[\theta_i]$ collected by sweeping through RFID orientations to estimate α, β, and c. The results of an example calibration are shown in Figure 5-2.

5.2.3 Position and Orientation Extraction

Having estimated the antenna polarizations, we move the RFID to a new location within the same localization space as used in the previous chapter and change its orientation. We run a new experiment and estimate the channel state information from two receive antennas per dimension. We then use each pair of computed channels

---

[1]Because we never defined a reference angle for θ, we need this initial parameter b in practical calibration to set a global coordinate system.

to estimate RFID position as described in Section 4.1.2 and use Equation 5.12 to compute orientation.
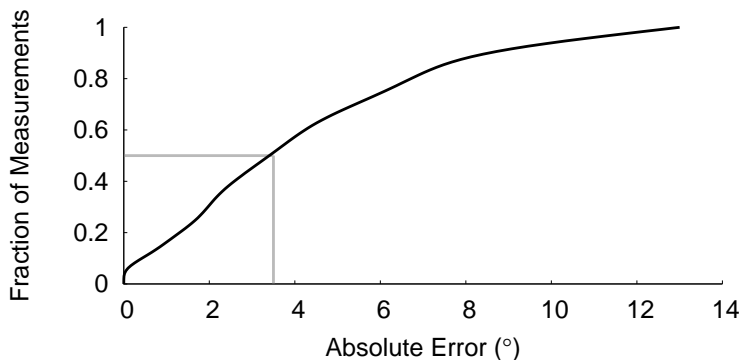
5.3   Results

Figure 5-3: **Orientation Extraction Accuracy.** We plot the CDF of RF-Reality's orientation extraction accuracy as we vary an RFID's position and orientation.

We focus on evaluating RF-Reality's orientation extraction algorithm in one dimension. In this evaluation, we begin by calibrating the antenna polarization parameters as described in Section 5.2. Next, we randomly place the RFID tag in the localization space on a measurement mat in front of the antennas. Then, we randomly choose an orientation between 0 and 360 degrees using a paper protractor. We collect measurements using RF-Reality and compare the results to the ground truth from the measurement mat and paper protractor. We plot the CDF of the measurement errors from 50 trials of both methods in Figure 5-3.

The figure demonstrates that RF-Reality estimates the orientation of a single RFID tag very accurately. Specifically, the median error is 3.5 degrees and the 90th percentile error is 8.3 degrees. These results demonstrate that RF-Reality can recover tag orientation with high accuracy independent of the location and in multipath environments.

Chapter 6

Conclusion

This thesis presents RF-Reality, a virtual and augmented reality system which leverages inexpensive RFID stickers to track objects even when they are hidden from view. RF-Reality builds on previous work in RF localization which tracks the location and orientation of RFID's. It presents new solutions to accurately estimate the position and orientation of an RFID tag in three dimensions anywhere within communication range, including tagged objects hidden behind furniture, and naturally extends to multiple RFID's. RF-Reality presents a fundamental leap in ability over vision based systems which are limited to tracking objects in line-of-sight, as well as an improvement over state-of-the-art RF localization systems.

6.1 Limitations

This implementation of RF-Reality exhibits four major limitations:

- Because RF-Reality constantly transmits a large-bandwidth OFDM symbol, the current implementation may not comply with FCC power regulations. If the bandwidth of the symbol is fit into one of the higher power public radio bands such as the ISM band, then RF-Reality would be FCC compliant. Restricting the bandwidth reduces accuracy and ability to deal with multipath, but transmitting at lower power either reduces range or increases latency.

- This thesis only evaluated RF-Reality within two meters from the transmit and receive antennas. It is desirable to extend the range and enable RFID localization over a wider area.

- While the proposed solutions for localization and orientation extraction have been implemented separately, in principle, they may be combined into a single system that would enable tracking the 3D positions and orientations of multiple tags at high frame rates.

- There exist several corner cases in which RF-Reality cannot retrieve accurate measurements of position or orientation. First, the tag will not power up if it is oriented such that the major axis of its antenna polarization vector is too close

to normal to that of the transmitting antenna (i.e. if the tag is oriented along the Ez dimension in Figure 4-2). There also exists a range of orientations at some locations for which the tag will also not power up. In our experiments, the tag would not power up when oriented between 140 and 150 degrees relative to the horizontal. Put simply, if the tag does not respond to the query command, RF-Reality will not be able to estimate its position or orientation.

6.2 Vision

RF-Reality's strengths lie in its ability to acquire accurate position and orientation estimates at very high frame rates. It requires no reference tags or prior knowledge of the environment, can handle multipath, and recovers from error by performing a new, independent location and orientation estimate in every frame. Because it operates entirely in the physical layer, it is transparent to EPC Gen2 protocol and can work with inexpensive, battery-less, off-the-shelf RFID tags.

We believe RF-Reality presents a new paradigm for commercial RFID localization. Beyond the application examples for VR/AR systems, rapid, accurate RFID localization has the potential to disrupt many industries. Warehouse inventory systems, sports analytics, robotics, and any field that involves object tracking can use RF-Reality to leverage the benefits of RF localization. Currently, RF-Reality exists as a new methodology for RFID localization, but it is plagued by practical limitations of general equipment designed for proof-of-concept demonstrations. We believe that by continuing to improve the efficiency of RF-Reality's underlying hardware and algorithm implementation, it promises an exciting future for commercial localization applications and virtual/augmented reality.

Bibliography

[1] EPC UHF Gen2 Air Interface Protocol. http://www.gs1.org/epcrfid/epc-rfid-uhf-air-interface-protocol/2-0-1.

[2] Ettus inc. http://www.ettus.com.

[3] Impinj r420. http://www.impinj.com. Impinj Inc.

[4] Intel X520. https://ark.intel.com. Intel X520.

[5] M6e. http://www.thingmagic.com. ThingMagic Inc.

[6] Minicircuits. https://www.minicircuits.com/.

[7] Mti mt-242025 antenna. https://www.atlasrfidstore.com/mti-mt-242025-trh-a-rhcp-outdoor-rfid-antenna-865-956-mhz/.

[8] Optitrack. http://www.optitrack.com.

[9] Vicon t-series. VICON.

[10] X-box kinect. http://www.xbox.com. Microsoft.

[11] The state of rfid implementation and its policy implications: An ieee-usa white paper. IEEE USA, 2009.

[12] Muhammad B Akbar, Cheng Qi, Mohammad Alhassoun, and Gregory D Durgin. Orientation sensing using backscattered phase from multi-antenna tag at 5.8 ghz. In *RFID (RFID), 2016 IEEE International Conference on*, pages 1–8. IEEE, 2016.

[13] Alien Technology Inc. ALN-9640 Squiggle Inlay. www.alientechnology.com.

[14] Sara Amendola, Luigi Bianchi, and Gaetano Marrocco. Movement detection of human body segments: Passive radio-frequency identification and machine-learning technologies. *IEEE Antennas and Propagation Magazine*, 57(3):23–37, 2015.

[15] Rubayet-E-Azim Anee and Nemai C Karmakar. Chipless rfid tag localization. *IEEE Transactions on Microwave Theory and Techniques*, 61(11):4008–4017, 2013.

[16] Daniel Arnitz, Klaus Witrisal, and Ulrich Muehlmann. Multifrequency continuous-wave radar approach to ranging in passive uhf rfid. *IEEE Transactions on Microwave Theory and Techniques*, 57(5):1398–1405, 2009.

[17] Ascension Technology. MotionStar. https://www.ascension-tech.com/.

[18] Salah Azzouzi, Markus Cremer, Uwe Dettmar, Rainer Kronberger, and Thomas Knie. New measurement results for the localization of uhf rfid transponders using an angle of arrival (aoa) approach. In *RFID (RFID), 2011 IEEE International Conference on*, pages 91–97. IEEE, 2011.

[19] Mathieu Bouet and Aldri L Dos Santos. Rfid tags: Positioning principles and localization techniques. In *Wireless Days, 2008. WD'08. 1st IFIP*, pages 1–5. IEEE, 2008.

[20] Mathieu Bouet and Guy Pujolle. A range-free 3-d localization method for rfid tags based on virtual landmarks. In *Personal, Indoor and Mobile Radio Communications, 2008. PIMRC 2008. IEEE 19th International Symposium on*, pages 1–5. IEEE, 2008.

[21] Kirti Chawla, Christopher McFarland, Gabriel Robins, and Connor Shope. Real-time rfid localization using rss. In *Localization and GNSS (ICL-GNSS), 2013 International Conference on*, pages 1–6. IEEE, 2013.

[22] Dana Cobzas and Hong Zhang. Cylindrical panoramic image-based model for robot localization. In *Intelligent Robots and Systems, 2001. Proceedings. 2001 IEEE/RSJ International Conference on*, volume 4, pages 1924–1930. IEEE, 2001.

[23] Jinsong Han, Chen Qian, Xing Wang, Dan Ma, Jizhong Zhao, Wei Xi, Zhiping Jiang, and Zhi Wang. Twins: Device-free object tracking using passive tags. *IEEE/ACM Transactions on Networking*, 24(3):1605–1617, 2016.

[24] Soonshin Han, HyungSoo Lim, and JangMyung Lee. An efficient localization scheme for a differential-driving mobile robot based on rfid system. *IEEE Transactions on Industrial Electronics*, 54(6):3362–3369, 2007.

[25] Cory Hekimian-Williams, Brandon Grant, Xiuwen Liu, Zhenghao Zhang, and Piyush Kumar. Accurate localization of rfid tags using phase difference. In *RFID, 2010 IEEE International Conference on*, pages 89–96. IEEE, 2010.

[26] Steve Hinske. Determining the position and orientation of multi-tagged objects using rfid technology. In *Pervasive Computing and Communications Workshops, 2007. PerCom Workshops' 07. Fifth Annual IEEE International Conference on*, pages 377–381. IEEE, 2007.

[27] HTC. Htc vive. https://www.vive.com/us/.

[28] C Hülsmeyer. Verfahren zur bestimmung der entfernung von metallischen gegen-
ständen (schiffen o. dgl.), deren gegenwart durch das verfahren nach patent
165546 festgestellt wird,âĂİ. *Deutschland Patent*, 169:154, 1904.

[29] John David Jackson. Classical electrodynamics, 1999.

[30] Uni Jyvaskyla. Rfid tags - global market size forecast 2016-2020. Technical
report, MIG, 2016.

[31] Paul A Kline. *Atomic clock augmentation for receivers using the global position-
ing system*. PhD thesis, Virginia Tech, 1997.

[32] Manikanta Kotaru and Sachin Katti. Position tracking for virtual reality using
commodity wifi. *IEEE CVPR*, 2017.

[33] Rasmus Krigslund, Strahinja Dosen, Petar Popovski, Jakob Lund Dideriksen,
Gert Frølund Pedersen, and Dario Farina. A novel technology for motion cap-
ture using passive uhf rfid tags. *IEEE Transactions on Biomedical Engineering*,
60(5):1453–1457, 2013.

[34] Rasmus Krigslund, Petar Popovski, and Gert F Pedersen. Orientation sensing
using multiple passive rfid tags. *IEEE Antennas and Wireless Propagation Let-
ters*, 11:176–179, 2012.

[35] Rasmus Krigslund, Petar Popovski, and Gert F Pedersen. 3d gesture recogni-
tion using passive rfid tags. In *Antennas and Propagation Society International
Symposium (APSURSI), 2013 IEEE*, pages 2307–2308. IEEE, 2013.

[36] Rasmus Krigslund, Petar Popovski, Gert F Pedersen, and Kristian Bank. Po-
tential of rfid systems to detect object orientation. In *Communications (ICC),
2011 IEEE International Conference on*, pages 1–5. IEEE, 2011.

[37] Rainer Kronberger, Thomas Knie, Roberto Leonardi, Uwe Dettmar, Markus
Cremer, and Salah Azzouzi. Uhf rfid localization system based on a phased array
antenna. In *Antennas and Propagation (APSURSI), 2011 IEEE International
Symposium on*, pages 525–528. IEEE, 2011.

[38] Ben JA Kröse, N Vlassis, and Roland Bunschoten. Omnidirectional vision for
appearance-based robot localization. In *Sensor based intelligent robots*, pages
39–50. Springer, 2002.

[39] Steven M LaValle, Anna Yershova, Max Katsev, and Michael Antonov. Head
tracking for the oculus rift. In *Robotics and Automation (ICRA), 2014 IEEE
International Conference on*, pages 187–194. IEEE, 2014.

[40] Xin Li, Yimin Zhang, and Moeness G Amin. Multifrequency-based range esti-
mation of rfid tags. In *RFID, 2009 IEEE International Conference on*, pages
147–154. IEEE, 2009.

[41] Ming K Lim, Witold Bahr, and Stephen CH Leung. Rfid in the warehouse: A literature analysis (1995–2010) of its applications, benefits, challenges and future trends. *International Journal of Production Economics*, 145(1):409–430, 2013.

[42] Tianci Liu, Lei Yang, Qiongzheng Lin, Yi Guo, and Yunhao Liu. Anchor-free backscatter positioning for rfid tags with high accuracy. In *INFOCOM, 2014 Proceedings IEEE*, pages 379–387. IEEE, 2014.

[43] WN Liu, LJ Zheng, DH Sun, XY Liao, M Zhao, JM Su, and YX Liu. Rfid-enabled real-time production management system for loncin motorcycle assembly line. *International Journal of Computer Integrated Manufacturing*, 25(1):86–99, 2012.

[44] Yunfei Ma, Xiaonan Hui, and Edwin C Kan. 3d real-time indoor localization via broadband nonlinear backscatter in passive devices with centimeter precision. In *Proceedings of the 22nd Annual International Conference on Mobile Computing and Networking*, pages 216–229. ACM, 2016.

[45] Yunfei Ma, Nicholas Selby, and Fadel Adib. Minding the billions: Ultrawideband localization for deployed rfid tags. *ACM MobiCom*, 2017.

[46] Guoqiang Mao, Barış Fidan, and Brian DO Anderson. Wireless sensor network localization techniques. *Computer networks*, 51(10):2529–2553, 2007.

[47] G Marrocco and F Amato. Self-sensing passive rfid: From theory to tag design and experimentation. In *Microwave Conference, 2009. EuMC 2009. European*, pages 001–004. IEEE, 2009.

[48] Gaetano Marrocco, Cecilia Occhiuzzi, and Francesco Amato. Sensor-oriented passive rfid. In *The Internet of Things*, pages 273–282. Springer, 2010.

[49] Andrew McWilliams. RFID: Technology, Applications, and Global Markets. BCC Research, 2016.

[50] Michael Meehan, Sharif Razzaque, Mary C Whitton, and Frederick P Brooks. Effect of latency on presence in stressful virtual environments. In *virtual reality, 2003. Proceedings. IEEE*, pages 141–148. IEEE, 2003.

[51] Meta Motion. Meta Motion Gypsy. https://www.metamotion.com.

[52] Robert Miesen, Fabian Kirsch, and Martin Vossiek. Holographic localization of passive uhf rfid transponders. In *RFID (RFID), 2011 IEEE International Conference on*, pages 32–37. IEEE, 2011.

[53] Lionel M Ni, Yunhao Liu, Yiu Cho Lau, and Abhishek P Patil. Landmarc: indoor location sensing using active rfid. *Wireless networks*, 10(6):701–710, 2004.

[54] Occulus. Occulus rift. https://www.oculus.com/rift/.

[55] Omni-ID. Omni-ID Exo. www.omni-id.com.

[56] Kyle Orland. How fast does "virtual reality" have to be to look like "actual reality"? Ars Technica, 2013. https://arstechnica.com/gaming/2013/01/how-fast-does-virtual-reality-have-to-be-to-look-like-actual-reality/.

[57] Michael Pelissier, Joni Jantunen, Bertrand Gomez, Jarmo Arponen, Gilles Masson, Serigne Dia, Jaakko Varteva, and Marjorie Gary. A 112 mb/s full duplex remotely-powered impulse-uwb rfid transceiver for wireless nv-memory applications. *IEEE Journal of Solid-State Circuits*, 46(4):916–927, 2011.

[58] Daniel Roetenberg, Henk Luinge, and Per Slycke. Xsens mvn: full 6dof human motion tracking using miniature inertial sensors. *Xsens Motion Technologies BV, Tech. Rep*, 2009.

[59] Jac Romme, Johan HC van den Heuvel, Guido Dolmans, G Selimis, Kathleen Philips, and Harmke de Groot. On remote rf-based orientation detection. In *Communications (ICC), 2013 IEEE International Conference on*, pages 4797–4801. IEEE, 2013.

[60] Longfei Shangguan and Kyle Jamieson. The design and implementation of a mobile rfid tag sorting robot. In *Proceedings of the 14th Annual International Conference on Mobile Systems, Applications, and Services*, pages 31–42. ACM, 2016.

[61] Longfei Shangguan and Kyle Jamieson. Leveraging electromagnetic polarization in a two-antenna whiteboard in the air. In *Proceedings of the 12th International on Conference on emerging Networking EXperiments and Technologies*, pages 443–456. ACM, 2016.

[62] Ali Asghar Nazari Shirehjini, Abdulsalam Yassine, and Shervin Shirmohammadi. An rfid-based position and orientation measurement system for mobile objects in intelligent environments. *IEEE Transactions on Instrumentation and Measurement*, 61(6):1664–1675, 2012.

[63] Robert Sim and Gregory Dudek. Learning and evaluating visual features for pose estimation. In *Computer Vision, 1999. The Proceedings of the Seventh IEEE International Conference on*, volume 2, pages 1217–1222. IEEE, 1999.

[64] Smartrac Group. Smartrac Shortdipole Inlay. www.smartrac-group.com.

[65] Sony. Playstation vr. https://www.playstation.com/en-us/explore/playstation-vr/.

[66] David H Staelin, Ann W Morgenthaler, and Jin Au Kong. *Electromagnetic waves*. Pearson Education India, 1994.

[67] Daniel Vlasic, Rolf Adelsberger, Giovanni Vannucci, John Barnwell, Markus Gross, Wojciech Matusik, and Jovan Popović. Practical motion capture in everyday surroundings. In *ACM transactions on graphics (TOG)*, volume 26, page 35. Acm, 2007.

[68] Jue Wang, Fadel Adib, Ross Knepper, Dina Katabi, and Daniela Rus. RF-Compass: Robot Object Manipulation Using RFIDs. In *ACM MobiCom*, 2013.

[69] Jue Wang and Dina Katabi. Dude, where's my card? rfid positioning that works with multipath and non-line of sight. In *ACM SIGCOMM*, 2013.

[70] Jue Wang, Deepak Vasisht, and Dina Katabi. Rf-idraw: virtual touch screen in the air using rf signals. In *ACM SIGCOMM*, 2015.

[71] Roy Want. An introduction to rfid technology. *IEEE pervasive computing*, 5(1):25–33, 2006.

[72] Teng Wei and Xinyu Zhang. Gyro in the air: tracking 3d orientation of batteryless internet-of-things. In *Proceedings of the 22nd Annual International Conference on Mobile Computing and Networking*, pages 55–68. ACM, 2016.

[73] Xsens. Xsens MVN. https://www.xsens.com/products/xsens-mvn/.

[74] Lei Yang, Yekui Chen, Xiang-Yang Li, Chaowei Xiao, Mo Li, and Yunhao Liu. Tagoram: Real-time tracking of mobile rfid tags to high precision using cots devices. In *Proceedings of the 20th annual international conference on Mobile computing and networking*, pages 237–248. ACM, 2014.

[75] Y. Yang and A. Fathy. Design and implementation of a low-cost real-time ultrawide band see-through-wall imaging radar system. In *IEEE/MTT-S International Microwave Symposium*, 2007.

[76] Chenming Zhou and Joshua D Griffin. Accurate phase-based ranging measurements for backscatter rfid tags. *IEEE Antennas and Wireless Propagation Letters*, 11:152–155, 2012.

[77] Junru Zhou, Hongjian Zhang, and Lingfei Mo. Two-dimension localization of passive rfid tags using aoa estimation. In *Instrumentation and Measurement Technology Conference (I2MTC), 2011 IEEE*, pages 1–5. IEEE, 2011.

[78] Junyi Zhou and Jing Shi. Rfid localization algorithms and applications-a review. *Journal of intelligent manufacturing*, 20(6):695–707, 2009.